Cellular Physiology and Biochemistry

Cell Physiol Biochem 2018;51:1616-1631
DOI: 10.1159/000495650
Published online: 29 November 2018
Accepted: 21 November 2018

Original Paper

Targeting P-Glycoprotein: Nelfinavir Reverses Adriamycin Resistance in K562/ADR Cells

Wei Liu[a] Qiang Meng[a,b] Yaoting Sun[c] Changyuan Wang[a,b] Xiaokui Huo[a,b] Zhihao Liu[a,b] Pengyuan Sun[a,b] Huijun Sun[a,b] Xiaodong Ma[a,b] Kexin Liu[a,b]

[a]Department of Clinical Pharmacology, College of Pharmacy, Dalian Medical University, Dalian, [b]Provincial Key Laboratory for Pharmacokinetics and Transport, Liaoning Dalian Medical University, Dalian, [c]Westlake Institute for Advanced Study, Hangzhou, China

Key Words
Nelfinavir (NFV) • Adriamycin (ADR) • Multidrug resistance (MDR) • P-glycoprotein (P-gp) • Chronic myelocytic leukemia (CML)

Abstract
Background/Aims: The emergence of multidrug resistance (MDR) caused by P-glycoprotein (P-gp) overexpression is a serious obstacle to the treatment of chronic myelocytic leukemia. In recent years, some clinical trials have shown that nelfinavir (NFV), a traditional anti-HIV drug, has anti-cancer effects. Some researchers have also shown NFV might be a potential P-gp inhibitor. This study is aimed at investigating whether nelfinavir can act as an MDR-reversal drug and to clarify its molecular mechanism as well. ***Methods:*** K562 and K562/ADR cell lines were applied in the study. Cytotoxicity was detected by CCK-8 reagents. Cell apoptosis was detected by flow cytometry and inverted fluorescence microscopy to detect the binding of apoptotic dyes to cells. Western blot was used to detect the expression of proteins. Drug-protein molecular docking simulation by using Sybyl-x 2.0 software. ***Results:*** Non-toxic concentrations of NFV (1.25–5 μM) could reverse Adriamycin (ADR), colchicine, paclitaxel, and imatinib resistance of K562/ADR cells, with reversal indexes of up to 10.8, 7.4, 57, and 9.3, respectively. NFV inhibited P-gp efflux function, as evidenced by the significant increase in the intracellular accumulation of ADR and Rho-123, without affecting P-gp protein and mRNA expression levels. Further ATP content detection and molecular docking simulations showed that NFV could decrease intracellular ATP content and has a high affinity with the active functional regions of P-gp, respectively. When co-administered with ADR, NFV increased intracellular reactive oxygen species as well as blocked the ERK/Akt signaling pathway, leading to cell

Qiang Meng
Kexin Liu, Prof. (Ph.D.)
Department of Clinical Pharmacology, College of Pharmacy, Dalian Medical University
9 West Section, Lvshun South Road, Lvshunkou District, Dalian 116044 (China)
Tel. +86 0411 8611 0407, Fax +86 0411 8611 0407, E-Mail mengq531@163.com; kexinliu@dlmedu.edu.cn

apoptosis. ***Conclusion:*** NFV inhibited P-gp function, decreased intracellular ATP content, and promoted cell apoptosis in K562/ADR cells, thereby reversing MDR. These findings encourage further animal and clinical MDR studies with a combination therapy consisting of NFV and chemotherapeutic drugs.

Introduction

Chronic myelocytic leukemia (CML) is a hematological tumor caused by abnormal proliferation of bone marrow granulocytes and their accumulation in the blood, accounting for 15% of all new cases of leukemia in western countries [1]. Before the emergence of tyrosine protein kinase inhibitors (TKIs), there were no particularly effective drugs for CML treatment [2, 3]. However, the emergence of resistance is a serious obstacle to CML chemotherapy. To resolve drug resistance, three generations of TKIs have been developed. The resistance mechanisms are complicated and can be summarized as follows: (1) BCR-ABL fusion gene duplication; (2) BCR-ABL gene mutations; (3) transmembrane transporter overexpression; and (4) changes in survival-related signaling pathways [4]. Among them, the overexpression of transmembrane transporters is the main cause of cancer cell resistance.

ABC-transporters comprise the largest family of transmembrane transporters. To date, 48 human ABC transporter genes have been found, and these genes have been divided into seven subfamilies, ABC subfamilies A to G [5]. These proteins pump a variety of endogenous substrates (such as inorganic anions, amino acids, peptides, and hydrophobic metabolites) or exogenous substrates (drugs and their metabolites) out of the cell, resulting in detoxification. However, this process also leads to a decrease in the intracellular drug concentration and results in drug resistance [6-8]. The p-glycoprotein (MDR1, P-gp), which is encoded by ABC subfamily B member 1 (ABCB1), is the most important and well-studied member of the ABC transporter family [9, 10]. Since P-gp has a wide range of substrates, when it is overexpressed in cancer cells, the cancer cells may be resistant to multiple drugs simultaneously, leading to multidrug resistance (MDR). The expression level of these transporters in cancer cells may determine the ability to confer drug resistance [11]. Down-regulating the expression of P-gp or inhibiting its function to overcome resistance has accordingly been an active research topic.

Nelfinavir (NFV), a protease inhibitor, was approved by the US Food and Drug Administration (FDA) for the treatment of AIDS in 1997 [12]. One study on the relationship between P-gp expression and function in AIDS patients and intracellular accumulation of NFV showed that NFV has significant exposure in patients› peripheral blood cells [13]. The accumulation may be related to NFV's inhibition of P-gp function. A regression study in 1998 found that protease inhibitors may partially alleviate the symptoms of Kaposi›s sarcoma [14]. These studies indicate that NFV can be used to reverse the drug resistance of P-gp-overexpressing cancer cells. If NFV can be used for the treatment of cancer, it will have many advantages. NFV has been used in the treatment of AIDS for more than 20 years, and its side effects, pharmacokinetic characteristics, and security are thoroughly understood. Indeed, NFV has only some common side effects, such as insulin resistance, hyperglycemia, and lipodystrophy, even at high doses [15].

In this study, we used NFV for the reversal of resistance in CML-resistant K562/ADR cells for the first time and explored its intrinsic molecular mechanism, which is expected to provide a new direction for CML resistance research.

Materials and Methods

Chemicals and antibodies

Nelfinavir mesylate (CAS:159989-65-8), Adriamycin (CAS:25316-40-9), colchicine (CAS:64-86-8), paclitaxel (CAS:33069-62-4), imatinib mesylate (CAS:220127-57-1), and cisplatin (CAS:15663-27-1)

were purchased from Dalian Meilun Biotech Co., Ltd. (Dalian, China). All of the chemicals were dissolved in dimethyl sulfoxide and diluted with RPMI medium 1640 (Thermo Fisher Scientific, Waltham, MA). Cell Counting Kit-8 (CCK-8) kits were obtained from Bimake (Houston, TX). Annexin V Apoptosis Detection Kit FITC and SYTOX™ Red Dead Cell Stain were purchased from Invitrogen, Ltd. (Carlsbad, CA). Antibodies against P-gp were purchased from Cell Signaling Technology (Danvers, MA). Antibodies against ERK1/2, p-ERK1/2, Akt, p-Akt caspase-3, and cleaved caspase-3 were also obtained from Cell Signaling Technology. Bcl-2 and bax were purchased from the Proteintech Group (Wuhan, China).

Cell culture

Human CML cells K562 and the related drug-resistant cell lines K562/ADR were purchased from Nanjing KeyGen Biotech Co., Ltd. (Nanjing, China), and they were cultured in RPMI medium 1640 with 10% fetal bovine serum (Thermo Fischer Scientific). Cells were incubated in 5% CO_2 and 95% humidity at 37°C. Cell passages and cell-resistance maintenance were carried out according to the manufacturer's instructions.

Cytotoxicity assay

Drug-induced cytotoxicity was detected with CCK-8 kits. Cells were seeded into 96-well plates at a density of 5×10^3 cells/well. After 24 h, cells were treated with the indicated drugs for 48 h. Then, 10 μL of CCK-8 reagent was added to each well and assayed by a microplate reader (Bio-Rad Laboratories, Hercules, CA) at 450 nm. The IC_{50} value was calculated using SPSS 22.0 (IBM Corp., Armonk, NY).

Intracellular accumulation of ADR

The cells were plated in 6-well plates at a density of 10^6 cells/well. After 24 h, cells were treated with the indicated drugs for 48 h. Then, 2 mL of 2 μM ADR was added to each well and incubated at 37°C for 45 min in the dark. After incubation, cells were immediately washed three times with ice-cold phosphate-buffered saline, and the cells were lysed with lysate and transferred to opaque 96-well plates for detection of fluorescent signals (495 nm excitation wavelength, 595 nm emission wavelength) using a multimode microplate reader (TriStar2, Berthold Technologies, Bad Wildbad, Germany).

Western blots

Sodium dodecyl sulfate-polyacrylamide gel electrophoresis was performed with 30-μg protein samples, which were loaded into gels. The final membranes were exposed to electrochemiluminescence and photographed using the ChemiDocTM XRS& Imaging system (Bio-Rad Laboratories). The grayscale of the bands was analyzed using Image Lab 3.0 (Bio-Rad Laboratories). The western blot protocol was carried out as previously described in detail [16].

Real-time quantitative PCR

Gene expression was determined by real-time quantitative PCR (RT-qPCR) following a previously published method [17]. Cells were treated with the indicated reagents for 48 h. The RNAiso Plus® Reagent Kit (Takara Biotechnology, Dalian, China) was used to extract total RNA, and 1 μg of total RNA was used for cDNA reverse transcription. cDNA templates were amplified and detected using the SYBR® Premix Ex TaqTM Kit (Takara Biotechnology) in the ABIPRISM® 7500 Real-Time PCR System (Applied Biosystems, Foster City, CA). Primers used for RT-qPCR were as follows: MDR1 forward primer 5′-GGAGCCTACTTGGTGGCACATAA-3′; MDR1 reverse primer 5′-TGGCATAGTCAGGAGCAAATGAAC-3′; GAPDH forward primer 5′-ACAACTTTGGTATCGTGGAAGG-3′; and GAPDH Reverse primer 5′-GCCATCACGCCACAGTTTC-3′.

Flow cytometry assay

Flow cytometry was used to detect the intracellular accumulation of RHO-123 (C2007, Beyotime Biotechnology, Shanghai, China), reactive oxygen species (ROS; S0033, Beyotime Biotechnology), Annexin V (BMS500FI, Invitrogen), and SYTOX™ Red (S34859, Invitrogen). The cells were plated in 6-well plates at a density of 10^6 cells/well. After 24 h, the cells were pretreated with the corresponding drugs for 48 h. Then, the cells were treated with different dyes according to the manufacturer's instructions and examined by flow cytometric analysis (FACScalibur, BD Biosciences, Franklin Lakes, NJ).

ATP content detection

The cells were plated in a 6-well plate at a density of 10^6 cells/well. After 24 h, cells were treated with the various drugs for 48 h. The cells were collected, and 300–500 μL of double distilled water was added. The cells were then homogenized and crushed in hot water. The resulting cell suspension was boiled in water for 10 min and vortexed for 1 min to extract intracellular ATP. An ATP content detection kit purchased from Nanjing Jiancheng Bioengineering Institute (Nanjing, China) was used to determine the level of ATP in the cells. Then, according to the instructions for the ATP content detection kit (Nanjing Jiancheng Bioengineering Institute), the intracellular ATP content was determined.

Molecular docking simulation

Molecular modelling was performed using Sybyl-x 2.0 software from Tripos Inc. (St. Louis, MO). The P-gp structure used for docking was obtained from the Protein Data Bank (PDB, http://www.rcsb.org; PDB ID, 4M2T and 6C0V). Verapamil, ADR, NFV, ATP, metformin, paclitaxel, colchicine, imatinib, cisplatin, tariquidar, laniquidar, and zosuquidar structures were obtained from zinc 15 (http://zinc15.org) [18]. The co-crystalized ligand and water molecules were removed from the structure, while H atoms were added and side chains were fixed during protein preparation. The Surflex-Dock (SFXC) docking mode was used, and the procedure was conducted as previously described [19]. Surflex-Dock was employed for the molecular docking study. Surflex-Dock scores (total scores) represent binding affinities.

Cell staining assay

The stage of apoptosis was analyzed using Hoechst 33342 (Beyotime Biotechnology), a dye for live-cell fluorescent staining of DNA. Mitochondrial membrane potential was detected using a JC-10 (Beijing Solarbio Science & Technology Co., Ltd., Beijing, China). When the mitochondrial membrane potential is low, JC-10 cannot accumulate in the matrix of the mitochondria, and in the form of a monomer, emits green fluorescence. The procedure followed the manufacturer's protocol instructions. Cells were observed using an inverted fluorescence microscope (OIS IX81, Olympus, Tokyo, Japan) in random microscopic fields. The relative fluorescence intensity was analyzed using ImageJ 1.46r.

Caspase-3 activity detection

The cells were plated in a 6-well plate at a density of 10^6 cells/well. After 24 h, cells were treated with the various drugs for 48 h. Caspase-3 activity was assayed using a Caspase 3 Colorimetric Assay Kit (KeyGen Biotech, Jiangsu, China) following the manufacturer's instructions.

Statistical analysis

Data are generally expressed as the mean ± SD. Significance was evaluated using two-tailed Student's *t*-tests or one-way analysis of variance using GraphPad Prism 5.01 (GraphPad Software Inc., La Jolla, CA) or SPSS 22.0, respectively. For all tests, a $P<0.05$ threshold was used to assess significance.

Results

NFV increases the sensitivity of K562/ADR cells to ADR

In order to detect the sensitizing effect of NFV on chemotherapeutic drugs in K562/ADR cells, a cytotoxicity assay was performed. K562/ADR cells were markedly resistant to ADR, with a resistance index of 63.6. Low concentrations of NFV (≤5 μM) had no influence on the growth of K562/ADR or K562 cell lines (Fig. 1A, B; Table 1). Therefore, non-toxic concentrations of 1.25, 2.5, and 5 μM NFV were selected to determine the effect on the half maximal inhibitory concentration (IC_{50}) of ADR. NFV was found to reduce the IC_{50} of ADR in a dose-dependent manner in K562/ADR cells, and its reversal index reached 10.8 (Fig. 1C, Table 1). However, NFV did not affect the sensitivity of the parental cell line to ADR (Fig. 1D). These data indicated that NFV could reverse the resistance of ADR by K562/ADR cells.

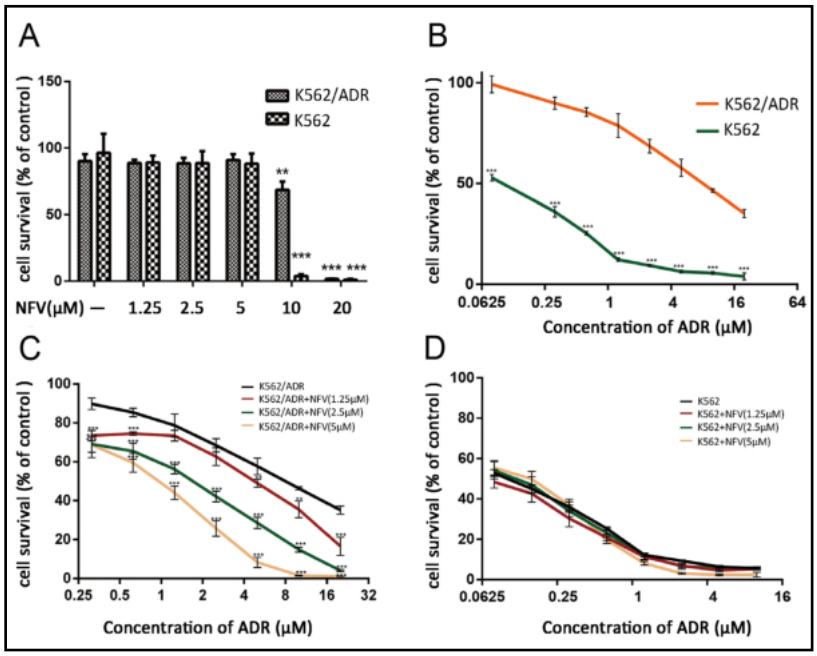

Fig. 1. Cytotoxicity of NFV and ADR in K562 and K562/ADR cells. Cells were treated with various concentrations of (A) NFV, (B) ADR, and (C, D) NFV combined with ADR for 48 h. The downward shift of the survival curves indicates that proliferation was inhibited. Columns are expressed as the mean ± SD. **P<0.01, ***P<0.001 relative to estimates obtained for the control group (A) and K562/ADR group (B, C).

NFV selectively increases the sensitivity of K562/ADR cells to drugs transported by P-gp

To further clarify the sensitization ability of NFV, four drugs (colchicine, paclitaxel, imatinib, and cisplatin) were used alone or co-administrated with NFV. Notably, NFV enhanced the sensitivity of K562/ADR cells to colchicine, paclitaxel, and imatinib in a dose-dependent manner with the highest reversal indexes of 7.4, 57, and 9.3, respectively, in the K562/ADR cell line. However, NFV did not have a significant influence on sensitization of cisplatin (Fig. 2, Table 2). These results indicated that NFV was selective for sensitizing chemotherapeutic drugs.

Table 1. IC_{50} values and reversal effect of NFV on ADR in K562 and K562/ADR cells. [a]IC_{50} values represent the mean ± SD of three independent experiments performed in triplicate. [b]Resistance Index was calculated by dividing the IC_{50} values of K562/ADR cells in the presence or absence of NFV by the IC_{50} values of K562 cells without NFV. [c]Reversal Index was calculated by dividing the values of the Resistance Index without NFV by the Resistance Index in the presence or absence of NFV. **P < 0.01 relative to the no NFV group

Drugs	IC_{50} ± SD[a] (μM)		Resistance Index[b]	Reversal Index[c]
	K562	K562/ADR		
ADR	0.13 ± 0.03	8.27 ± 0.59	63.6	1
ADR+NFV (1.25 μM)	0.11 ± 0.06	4.51 ± 0.44**	41	1.6
ADR+NFV (2.5 μM)	0.14 ± 0.02	1.32 ± 0.21**	9.4	6.8
ADR+NFV (5 μM)	0.14 + 0.01	0.82 ± 0.09**	5.9	10.8

NFV inhibits the P-gp function rather than expression, thus increasing intracellular ADR accumulation

To elucidate the mechanism of NFV reversal of ADR resistance, an ADR intracellular accumulation assay was performed. In K562/ADR cells, NFV increased the fluorescence signal of ADR in a dose-dependent manner. When the NFV concentration reached 5 μM, the intracellular accumulation of ADR was even higher than that of the positive control-verapamil (VRP) group. The ADR fluorescence signal did not change significantly as NFV increased in the K562 cell line (Fig. 3A). The effect of NFV on P-gp expression, MDR1 level, and efflux function were then assessed using western blot, RT-qPCR, and Rho-123 intracellular accumulation assays, respectively. NFV did not alter the expression of P-gp or the level of MDR1 transcripts, which encode P-gp (Fig. 3B). NFV increased the intracellular accumulation of Rho-123 in a dose-dependent manner, which suggested the inhibition of the P-gp efflux function. However, in sensitive cell lines, NFV, and VRP did not alter the intracellular accumulation of

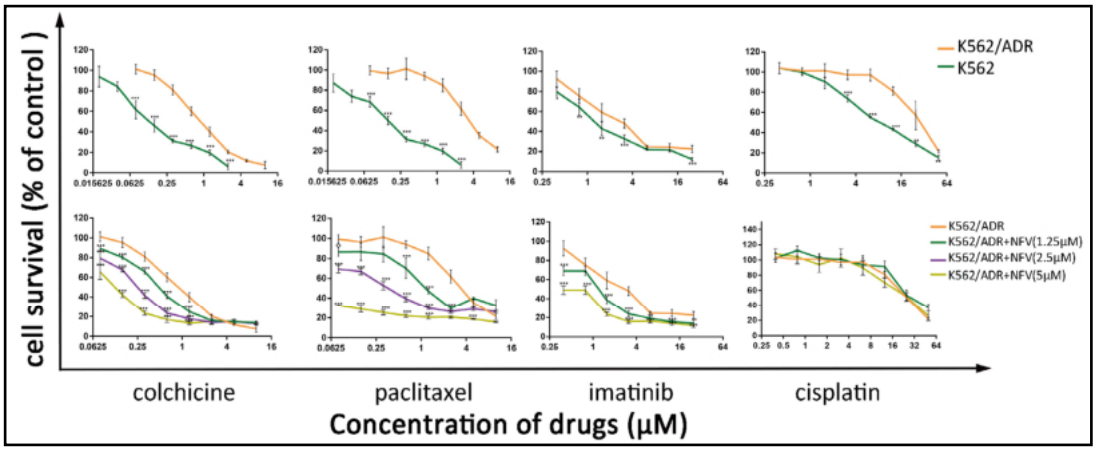

Fig. 2. Cytotoxicity of colchicine, paclitaxel, imatinib, and cisplatin in K562 and K562/ADR cells. Cells were treated with various concentrations of colchicine, paclitaxel, imatinib, and cisplatin individually or in combination with different concentrations of NFV for 48 h. Columns are expressed as the mean ± SD. *P<0.05, **P<0.01, ***P<0.001 relative to estimates obtained for the K562/ADR group.

Rho-123 (Fig. 3C, D). Taken together, these results suggested that NFV reverses the drug resistance of ADR by inhibiting the efflux function of P-gp and leading to an increase of the intracellular ADR concentration.

ATP is involved in the reversal of MDR by NFV

To further examine the deep mechanism of the reversal effect, we first examined the effects of NFV on mitochondria. The mitochondrial membrane was depolarized by NFV according to the green fluorescence increase observed (Fig. 4D). The intracellular ATP content was significantly decreased after NFV administration in K562/ADR cells (Fig. 4A). In order to investigate the effect of ATP content on the reversal ability of NFV, we changed the intracellular ATP content through induction by 1.25, 2.5, and 4.5 g/L glucose (Fig. 4B). The higher the glucose concentration, the higher the IC_{50} value of the ADR, indicating that the NFV reversal ability was weaker (Fig. 4C). These data suggest that NFV-induced ATP reduction was associated with the ultimate reversal of ADR resistance observed.

Table 2. IC_{50} values and reversal effect of NFV on chemotherapeutic drugs in K562 and K562/ADR cells. [a]IC_{50} values represent the mean ± SD of three independent experiments performed in triplicate. [b]Resistance Index was calculated by dividing the IC_{50} values of K562/ADR cells in the presence or absence of NFV by the IC_{50} values of K562 cells without NFV. [c]Reversal Index was calculated by dividing the values of Resistance Index without NFV by the Resistance Index in the presence or absence of NFV. **P < 0.01 relative to the no NFV group

Drugs	IC_{50} ± SD[a] (μM)		Resistance Index[b]	Reversal Index[c]
	K562	K562/ADR		
Colchicine	0.16 ± 0.02	0.95 ± 0.12	5.9	1
+NFV (1.25 μM)		0.53 ± 0.08**	3.3	1.8
+NFV (2.5 μM)		0.27 ± 0.05**	1.7	3.4
+NFV (5 μM)		0.13 ± 0.03**	0.8	7.4
paclitaxel	0.1627 ± 0.02	3.9 ± 0.65	24.4	1
+NFV (1.25 μM)		1.6 ± 0.35**	10	2.4
+NFV (2.5 μM)		0.43 ± 0.11**	2.7	9
+NFV (5 μM)		0.07 ± 0.02**	0.43	57
imatinib	1.48 ± 0.21	2.9 ± 0.64	1.96	1
+NFV (1.25 μM)		1.2 ± 0.15**	0.67	2.9
+NFV (5 μM)		0.56 ± 0.11**	0.21	9.3
cisplatin	9.5 ± 1.05	34.5 ± 8.3	3.6	1
+NFV (1.25 μM)		41.2 ± 11	4.3	0.8
+NFV (5 μM)		27.8 ± 7.2	2.9	1.2

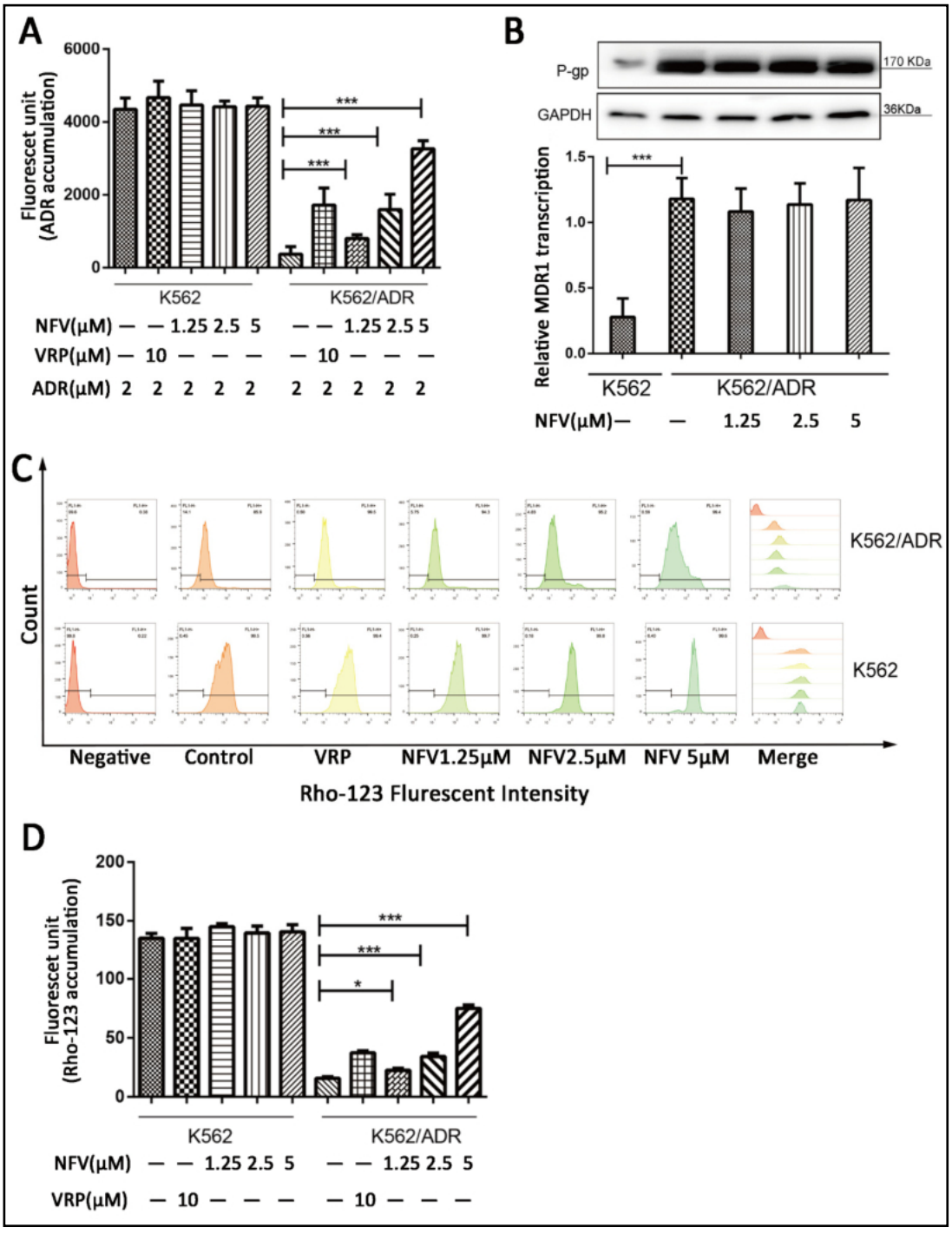

Fig. 3. Intracellular accumulation of ADR and effect of NFV on expression and function of P-gp in K562 and K562/ADR cells. (A) Intracellular accumulation was detected by a multimode microplate reader. (B) P-gp and P-gp mRNA (MDR1) expression was detected by western blot and RT-qPCR, respectively. (C) Accumulation of Rho-123 was determined by flow cytometry. (D) Fluorescence intensity analysis of (C). Columns are expressed as the mean ± SD. *P<0.05, ***P<0.001.

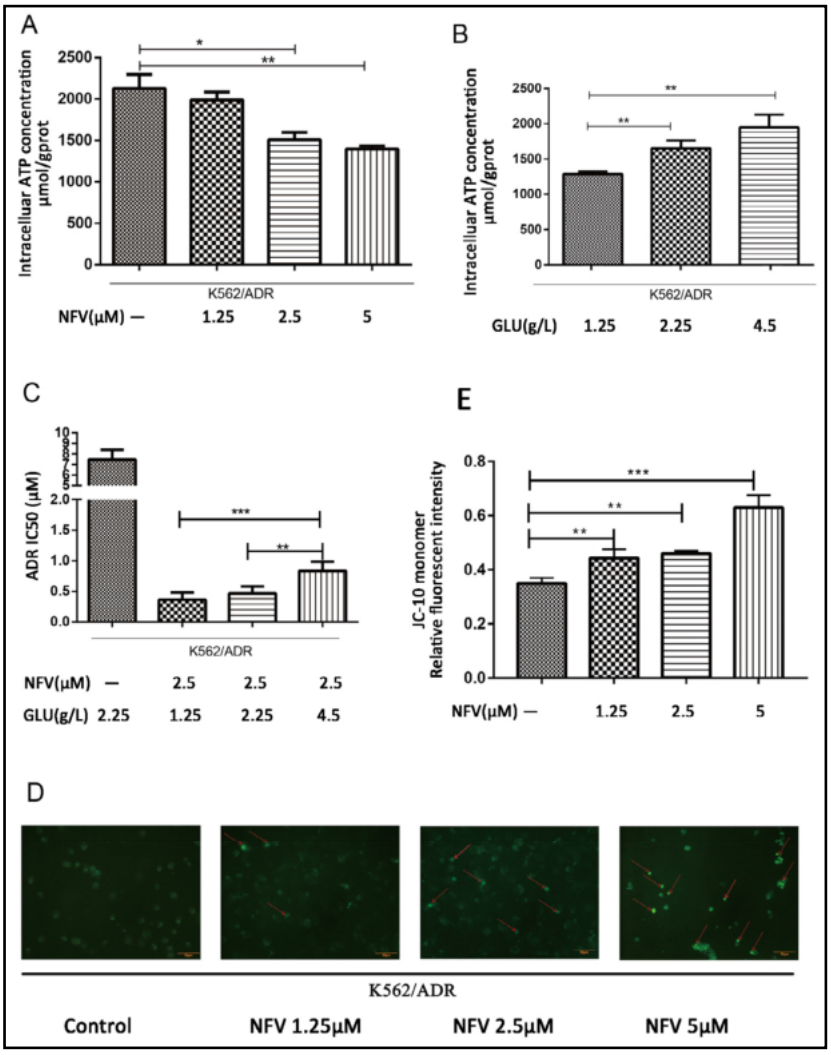

Fig. 4. Measurement of intracellular ATP content and mitochondrial membrane potential. (A, B) The effect of NFV and glucose on intracellular ATP content. The final determined ATP content is corrected with the corresponding protein concentration. (C) The effect of NFV and glucose on ADR IC_{50} values. (D) Detection of mitochondrial membrane potential by JC-10 fluorescent probe and the analysis of relative fluorescence intensity of JC-10 monomers. JC-10 monomers are indicated by red arrows. Columns are expressed as the mean ± SD. *P<0.05, **P<0.01, ***P<0.001.

Molecular docking analysis of the binding of NFV with P-gp

To elucidate the interaction between NFV and P-gp, P-gp's X-ray diffraction and electron microscopy structure (PDB ID: 4M2T and 6C0V, respectively) was assessed in a molecular docking simulation. NFV, VRP, ADR, paclitaxel, colchicine, and imatinib had strong affinities with 4M2T, with molecular docking simulation scores of 7.85, 6.91, 6.52, 6.31, 5.2, and 9.61, respectively. However, metformin and cisplatin, which are non-P-gp substrates, showed weak affinities with 4M2T, with binding ability scores of 2.31 and 4.08, respectively [20]. In addition, VRP and ADR had the same amino acid residue binding site for 4M2T, A/GLN986; NFV and ADR also had the same amino acid residue binding site for 4M2T, A/GLN721 (Fig. 5A, Table 3). ATP was inferred to form 13 intermolecular hydrogen bonds with 6C0V through 11 amino acid residues at a score of 10.28. NFV and tariquidar, a third-generation P-gp inhibitor, inhibited P-gp indirectly by blocking the activity of ATP synthase, and it had similar affinities with 6C0V, having scores of 9.52 and 9.88, respectively [21]. Moreover, NFV and ATP had the same amino acid residue binding site, A/ARG404; tariquidar and ATP also have the same amino acid residue binding site, A/SER434, which binds to 6C0V (Fig. 5B, Table 3). These shared binding sites may competitively inhibit the binding of ATP to P-gp NBD and indirectly inhibit the efflux function of P-gp.

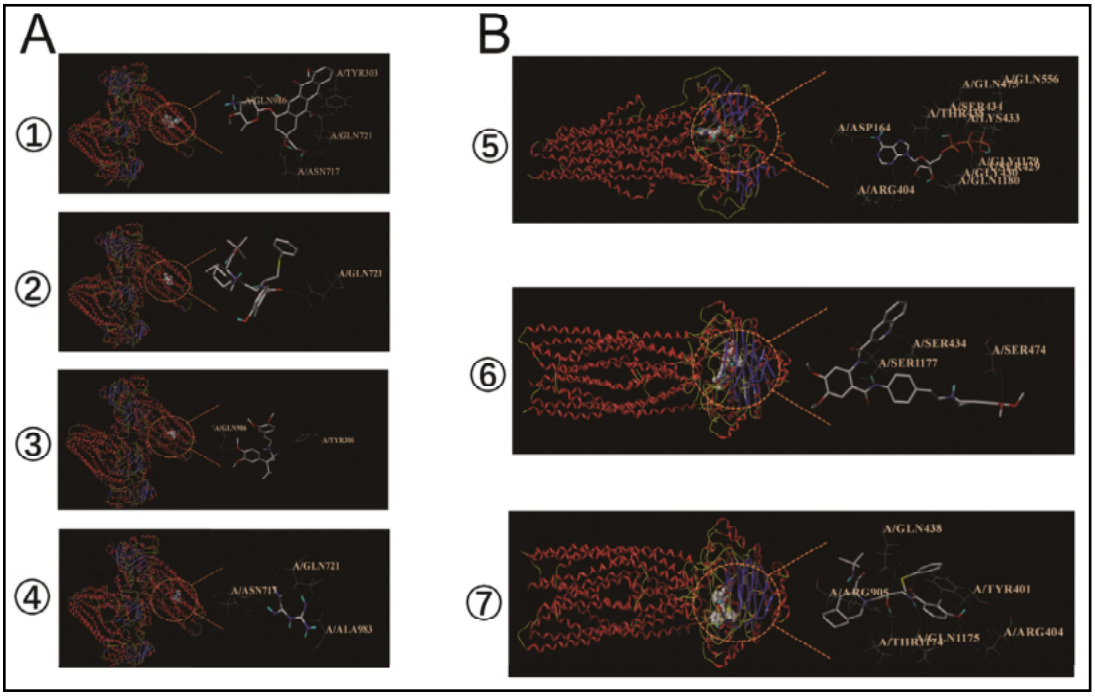

Fig. 5. Molecule docking simulations of compounds with 4M2T and 6C0V. (A) ADR, NFV, VRP, and metformin (labeled 1, 2, 3, and 4, respectively) in the active area of 4M2T. (B) ATP, NFV, and tariquidar (labeled 5, 6, and 7, respectively) in the active area of 4M2T. The orange dotted line represents the intermolecular hydrogen bond between the compound and the amino acid residues.

Table 3. Molecule docking simulation of the compounds with 4M2T or 6C0V

Compounds	Binding sites	Number of hydrogen bonds	Score
	4M2T		
VRP	A/GLN986, A/TYR306	2	7.85
ADR	A/ASN717, A/GLN986 A/TYR303, A/GLN721	7	6.91
NFV	A/GLN721	1	6.52
paclitaxel	A/TYR306, AGLN/721	2`	6.31
colchicine	B/GLN721		5.2
imatinib	A/GLN 721	1	9.61
cisplatin	A/ASN717, A/GLN843	2	4.08
Metformin	A/GLN721, A/ASN717 A/ALA983	3	2.31
	6C0V		
ATP	A/GLY1179, A/SER429, A/GLY430, A/GLN475, A/SER434, A/TYR435 A/GLN556, A/LYS433, A/GLN1180 A/ARG404, A/ASP164	13	10.28
NFV	A/ARG905, A/THR1174, A/TYR401, A/GLN438, A/GLN1175, A/ARG404	7	9.52
tariquidar	A/SER474, A/SER434, A/SER1177	3	9.88
laniquidar	A/ARG905, A/SER474	2	9.95
zosuquidar	A/THR1174	1	7.27

NFV combined with ADR increased intracellular ROS and blocked the ERK/Akt signaling pathway

Flow cytometry and western blot assays were performed to detect changes in intracellular ROS and related protein expression, which indicated the effects of NFV on the intracellular environment and survival signal pathway. A combination of NFV and ADR lead to a significant elevation in intracellular ROS compared to NFV or ADR administered alone (Fig. 6A, B). In addition, we examined the effect of NFV on the expression of total and phosphorylated Akt and ERK 1/2 in K562/ADR cells. When NFV or ADR was administered alone, the expression of total and phosphorylated Akt and ERK exhibited no alteration. When combined, NFV and ADR administration were associated with significant reductions in phosphorylated Akt and ERK 1/2 expression (Fig. 6C, D). These results indicated that enhanced cytotoxic responses by co-treatment with NFV and ADR in K562/ADR was associated with an increase of ROS and inhibition of the ERK/Akt pathways.

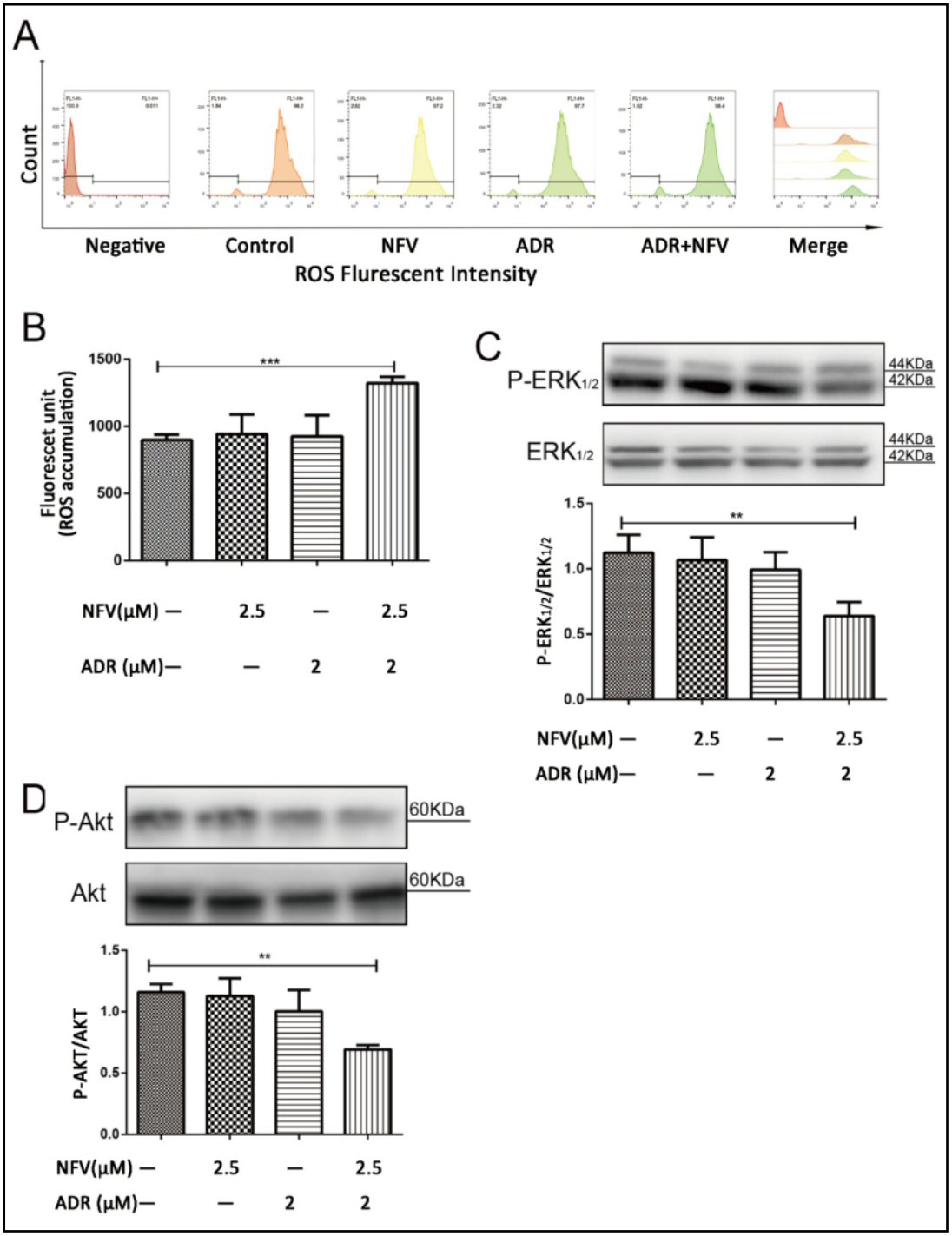

Fig. 6. Intracellular accumulation of ROS and protein levels of P-ERK1/2, ERK1/2, Akt, and p-Akt in K562/ADR cells. (A) The intracellular accumulation of ROS in K562/ADR was detected by flow cytometry. (B) Fluorescence intensity analysis of (A). (C) P-ERK1/2 and ERK1/2 protein expression level. (D) Akt and P-Akt protein expression level. Relative expression of phosphorylated forms was calculated by division of the expression of the phosphorylated form by the total form expression level. Columns are expressed as the mean ± SD. *P<0.05, **P<0.01, ***P<0.001.

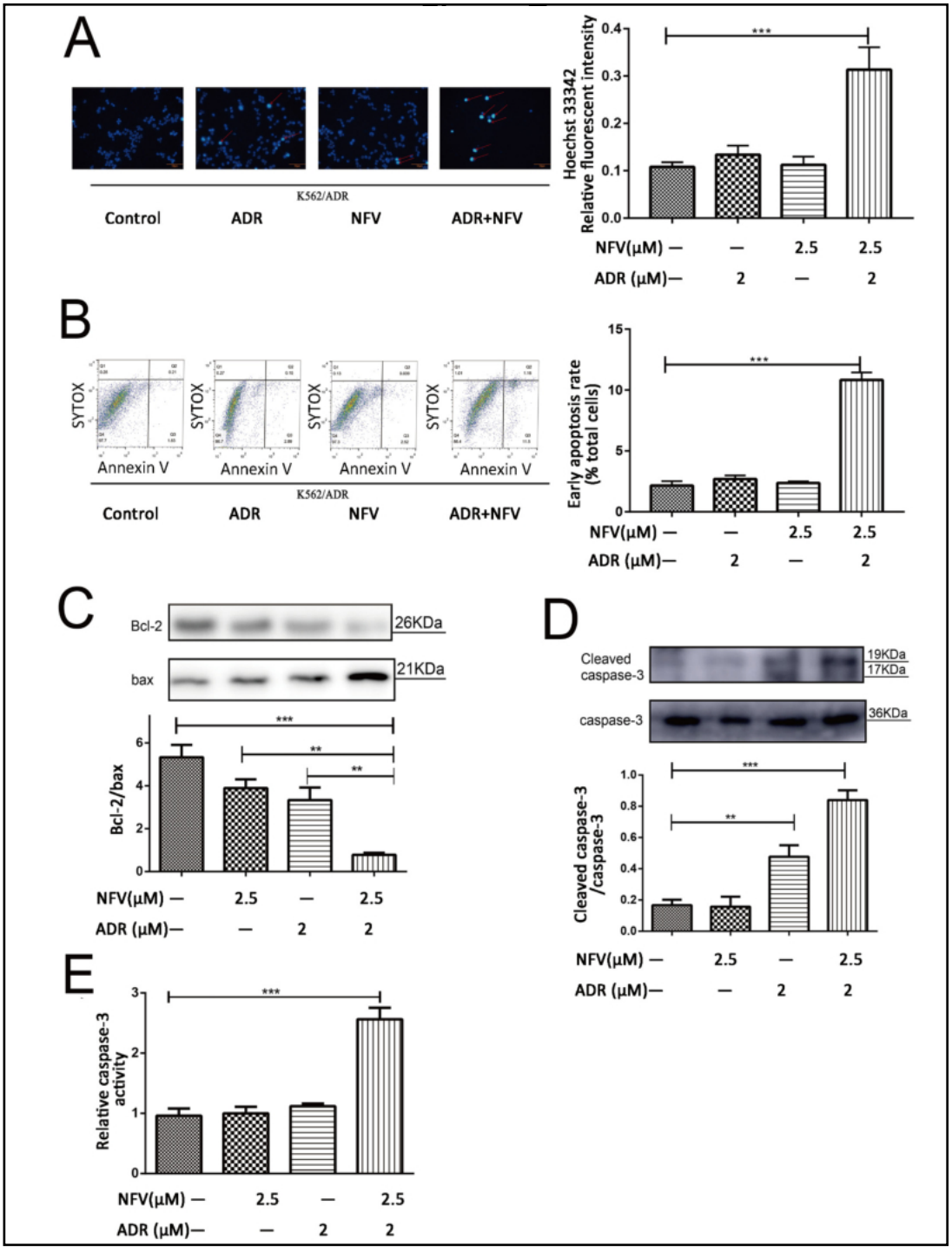

Fig. 7. A combination of NFV and ADR strengthened apoptosis induced by ADR in K562/ADR cells (A) K562/ADR cells were stained with Hoechst 33342 after pre-treatment and observed with an inverted fluorescence microscope. Nuclear fragmentation is indicated by red arrows. Relative fluorescence intensity of Hoechst 33342 was analyzed using ImageJ. (B) Annexin V/SYTOX-stained cells were examined by flow cytometry, and the Q3 quadrant indicates the ratio of cells in early apoptosis. (D) Protein expression and (E) activity of caspase-3 were determined by western blot assay and corresponding kits. (C) Protein expression bands of Bcl-2 and bax from western blots and the Bcl-2/bax ratio calculated by dividing the Bcl-2 expression level by the bax expression level. Columns and values were expressed as the mean ± SD. *P<0.05, **P<0.01, ***P<0.001.

Combination of NFV combined with ADR induces apoptosis in K562/ADR cells

To reveal the ultimate mechanism of anti-proliferation induced by NFV combined with ADR, cell apoptosis and the expression and activity of related proteins were measured. First, Hoechst33342 staining indicated nucleus changes. These results showed that the degree of nuclear fragmentation in the drug combination groups was significantly increased, which indicated that cell apoptosis occurred at a higher rate in the drug combination groups relative to the single-drug groups (Fig. 7A). Second, we detected the proportions of cells exhibiting early cell apoptosis by flow cytometry. In order to avoid fluorescence interference produced by Adriamycin, we used the far-infrared luminescent dye SYTOX Red (635 nm excitation wavelength, 658 nm emission wavelength) and Annexin V for detection.

The result showed that early cell apoptosis was significantly increased in the drug combination groups (Fig. 7B). In addition, the expression of the Bcl apoptotic protein family and the apoptosis-executing protein caspase-3 were examined by western blot. Compared with the single-drug groups, the expression of cleaved-caspase 3 was significantly increased in the combined NFV and ADR group, and the ratio of anti-apoptotic protein Bcl-2 to pro-apoptotic protein bax was significantly decreased. The results of the caspase-3 activity assay also confirmed that the drug combination significantly activated caspase-3 to promote apoptosis (Fig. 7C, D, E). These results indicate that NFV can increase the sensitivity of K562/ADR to ADR and increase apoptosis of drug-resistant cells to reverse ADR resistance.

Discussion

MDR has hindered the effectiveness chemotherapy of leukemia and other cancers. In contrast with the treatment of solid tumors, leukemia is mainly treated with chemotherapy combined with bone marrow transplantation. The emergence of molecularly targeted drugs is a milestone in CML therapy, which has led to a 10-year overall survival rate of 84% in patients with CML [22, 23]. However, the gradually developed drug resistance associated with CML treatment has attracted the attention of researchers, and one of the causes of drug resistance is P-gp overexpression [4, 24]. K562/ADR cells are a traditional model for studying drug resistance in CML cells. Targeting P-gp to reverse cancer cell resistance is a component of the most widely studied strategies. Four generations of studies on P-gp inhibitors have been performed. However, owing to side effects and low inhibitory ability, there is no drug that can be satisfactorily applied in clinical practice [25-28]. Our experimental results show that NFV can avoid these two points very well. First, at concentrations of 5 μM and below, NFV did not have significant cytotoxicity, while the reversal index was up to 10.8 (Fig. 1A, Table 1), indicating that NFV is a potent reversal agent. Second, one early study showed that single doses (100–800 mg) or multiple doses (800–900 mg) of NFV per day were well tolerated. When NFV was administered orally with food to healthy human volunteers at a dose of 800 mg, the Cmax value was 5.69 ± 1.05 μM [29]. Another phase I clinical trial of NFV-treated solid tumors showed that the drug concentration reached 21 μM and was still well tolerated in subjects at the 2.5 times the FDA-approved dose [30]. Therefore, experimental *in vitro* data shows that NFV can significantly enhance the sensitivity of drug-resistant cells to ADR, and this concentration of NFV is physiologically easy to achieve. In addition, we also observed that when the concentration of NFV is greater than 5 μM, it demonstrates obvious toxicity to k562 cells (Fig. 1A). Therefore, whether NFV, a traditional anti-AIDS drug, can be a new type of anti-tumor drug is worthy of further study.

Drug resistance to multiple chemotherapeutic drugs at the same time is one of the main causes of chemotherapy failure [31]. In addition to resistance to ADR, K562/ADR cells also showed different degrees of resistance to colchicine, paclitaxel, imatinib, and cisplatin, which is one of the most prominent features of MDR (Fig. 2, Table 2). It is well known that colchicine, paclitaxel, and imatinib are all substrates for P-gp, and cisplatin is neither an inhibitor nor a substrate of P-gp [32-35]. NFV can selectively reverse the resistance of drugs transported by P-gp; for the non-P-gp substrate drug cisplatin, NFV does not radically change

its drug resistance (Fig. 2, Table 2). Therefore, we speculate that NFV exerts a reversal effect by targeting P-gp. In addition, the results of cisplatin also suggested that the emergence of drug resistance in K562/ADR cells is a complex issue.

Intracellular accumulation of ADR showed that NFV increased the content of intracellular ADR in a dose-dependent manner (Fig. 3A). These experiments demonstrate that NFV reverses resistance by increasing the content of intracellular drugs. ADR is a substrate of P-gp, and P-gp is overexpressed in K562/ADR cells, so we speculate that NFV inhibits P-gp and leads to an increase in intracellular drugs [36]. Therefore, we examined the interaction between NFV and P-gp through both the function and expression of P-gp. First, we found that P-gp expression and its gene transcript levels were not down-regulated after K562/ADR cells were administered NFV for 48 h. Functionally, NFV inhibited the efflux of the P-gp-specific fluorogenic substrate Rho-123 in a dose-dependent manner, which indicates NFV inhibited P-gp efflux function (Fig. 3B, C, D).

P-gp transports one molecule of the substrate across the membrane, requiring two molecules of ATP to provide energy [37]. If the energy supply is insufficient, the function of P-gp is inhibited [38, 39]. The mitochondrion is the "powerhouse" of eukaryotic cells and the principal organelle involved in the production of ATP. Our study found that NFV can reduce mitochondrial membrane potential (Fig. 4D). This phenomenon is also called mitochondrial permeability transition (MPT), in which some low molecular weight solutes (<1.5 kDa) are infiltrated into the mitochondrial matrix, affecting its structure and leading to mitochondrial function collapse [40]. For the "powerhouse" of the cell, this will inevitably affect the intracellular ATP content, which is consistent with our experimental results (Fig. 4A). When the intracellular ATP content increases, the reversal ability of NFV is weakened, which also indirectly indicates that the decrease in ATP content caused by NFV is one of the reasons for the observed reversal of drug resistance (Fig. 4B, C).

The basic structure of P-gp contains four core active regions, namely two hydrophilic nucleotide-binding domains (NBD) located in the cytoplasm that are responsible for binding to ATP and two hydrophobic transmembrane domains (TMD) that are responsible for binding to the substrate for P-gp transport [37, 41]. For 4M2T, a corrected structure of mouse P-gp bound to QZ59-SSS, the corrected position of TMD4, which forms the frame of a portal for drug entry. The drug translocation pathway of Mouse P-gp is 96% identical to human P-gp and is enriched for aromatic residues that likely play a collective role in allowing a high degree of poly-specific substrate recognition [42]. Therefore, we chose 4M2T as a protein stereo structure model for binding drugs to TMD. For 6C0V, a new molecular structure of human P-gp was inferred to have an ATP-bound, outward-facing conformation. The researchers further found that the binding of ATP and NBD sites promoted drug release rather than hydrolysis [43]. Therefore, we chose 6C0V as a protein stereo structure model for binding drugs to NBD. Results of molecular docking simulation explain the interaction of NFV with P-gp active functional regions. NFV has a strong binding ability to TMD and NBD, and it has a common binding site with ADR and ATP in the corresponding functional regions. These common binding sites may result in inhibition of the binding of P-gp to drugs or ATP, resulting in the efflux function of P-gp being affected (Fig. 5). In addition, we also found that VRP and ADR have the same binding site. Similarly, Tariquidar and ATP also have the same binding site, but these binding sites differ from those of NFV. If these particular amino acid residues can be mutated, the binding of P-gp to the drug is blocked, and the normal physiological function of P-gp is not affected, which may eventually solve the drug resistance problem caused by P-gp.

ROS, as signaling molecules, participate in tumor cell proliferation inhibition, autophagy, apoptosis, and drug resistance. ROS inhibit cell proliferation mainly through mitogen-associated protein kinases (MAPKs)[44]. MAPKs comprise a highly conserved family of serine/threonine protein kinases that plays a role in many essential cellular processes. The MAPK family includes extracellular signal-regulated kinases 1 and 2 (ERK1/2), JNK, Erk5, and others [45]. Protein Kinase B, also known as Akt, regulates multiple biological processes, including cell survival, proliferation, growth, and glycogen metabolism [46].

The activation of the PI3K/Akt and MAPK/ERK pathway is related to the development of MDR in cancer cells [47-49]. Cancer cells are not sensitive to chemotherapeutic drugs, leading to a reduction in cell death caused by chemotherapeutic drugs, which leads to the emergence of drug resistance. After the development of drug resistance in cells, changes in the proteins that are related to the drug-induced survival signal pathway are not obvious. The results showed that 2 μM ADR alone did not significantly change the expression of total or phosphorylated ERK/Akt and intracellular ROS generation. When ADR was combined with NFV, the survival pathway was blocked, and ADR-induced apoptosis was significantly increased. Hoechst33342 staining, AV/SYTOX double staining, caspase-3activity detection, and Bcl-2/bax protein expression assays confirmed this trend (Fig. 6, Fig. 7).

Conclusion

As an "off-the-shelf" drug, NFV is effective in reversing K562/ADR cell resistance below physiologically acceptable concentrations. NFV can inhibit the function of P-gp by inducing intracellular ATP content and competitive drugs with ATP and P-gp binding sites, thereby increasing intracellular accumulation of ADR and exerting a reversal effect. The combination of NFV and ADR leads to an increase of ROS, blocking the ERK/Akt signaling pathway to increase apoptosis.

Acknowledgements

The work was supported by grants from the National Natural Science Foundation of China (Nos. 81473280, U1608283, and 81874324). The authors have no ethical conflicts to disclose. Kexin Liu and Qiang Meng contributed to the conception of the study. Wei Liu, Kexin Liu, and Qiang Meng contributed significantly to analysis and manuscript preparation. Wei Liu performed the data analyses and wrote the manuscript. Yaoting Sun, Changyuan Wang, Xiaokui Huo, Zhihao Liu, Pengyuan Sun, Huijun Sun, and Xiaodong Ma helped perform the analysis with constructive discussions.

Disclosure Statement

The authors have no conflicts of interest to declare.

References

1 Apperley JF: Chronic myeloid leukaemia. The Lancet 2015;385:1447-1459.
2 Soverini S, Mancini M, Bavaro L, Cavo M, Martinelli G: Chronic myeloid leukemia: the paradigm of targeting oncogenic tyrosine kinase signaling and counteracting resistance for successful cancer therapy. Molecular Cancer 2018;17:49.
3 Rowley JD: A New Consistent Chromosomal Abnormality in Chronic Myelogenous Leukaemia identified by Quinacrine Fluorescence and Giemsa Staining. Nature 1973;243:290-293.
4 Bixby D, Talpaz M: Seeking the causes and solutions to imatinib-resistance in chronic myeloid leukemia. Leukemia 2011;25:7-22.
5 Ambudkar SV, Kimchisarfaty C, Sauna ZE, Gottesman MM: P-glycoprotein: from genomics to mechanism. Oncogene 2003;22:7468-7485.
6 Rees DC, Johnson E, Lewinson O: ABC transporters: the power to change. Nat Rev Mol Cell Biol 2009;10:218-227.
7 Tarling EJ: Role of ABC transporters in lipid transport and human disease. Trends in Endocrinology & Metabolism Tem 2013;24:342-350.

8 Ter BJ, Guskov A, Slotboom DJ: Structural diversity of ABC transporters. Journal of General Physiology 2014;143:419-435.
9 Shaffer BC, Gillet JP, Patel C, Baer MR, Bates SE, Gottesman MM: Drug resistance: Still a daunting challenge to the successful treatment of AML. Drug Resistance Updates 2012;15:62-69.
10 Tang R, Faussat AM, Majdak P, Perrot JY, Chaoui D, Legrand O, Marie JP: Valproic acid inhibits proliferation and induces apoptosis in acute myeloid leukemia cells expressing P-gp and MRP1 Leukemia 2004;18:1246-1251.
11 Mlejnek P, Kosztyu P, Dolezel P, Bates SE, Ruzickova E: Reversal of ABCB1 mediated efflux by imatinib and nilotinib in cells expressing various transporter levels. Chem Biol Interact 2017;273:171-179.
12 Pai V, Nahata M: Nelfinavir mesylate: a protease inhibitor. Annals of Pharmacotherapy 1999;33:325-339.
13 Hennessy M, Clarke S, Spiers JP, Kelleher D, Mulcahy F, Hoggard P, Back D, Barry M: Intracellular accumulation of nelfinavir and its relationship to P-glycoprotein expression and function in HIV-infected patients. Antiviral Therapy 2004;9:115-122.
14 Lebbé C, Blum L, Pellet C, Blanchard G, Vérola O, Morel P, Danne O, Calvo F: Clinical and biological impact of antiretroviral therapy with protease inhibitors on HIV-related Kaposi's sarcoma. Aids 1998;12:45-49.
15 Shim JS, Liu JO: Recent Advances in Drug Repositioning for the Discovery of New Anticancer Drugs. International Journal of Biological Sciences 2014;10:654-663.
16 Zhang Y, Wang CY, Duan YJ, Huo XK, Meng Q, Liu ZH, Sun HJ, Ma XD, Liu KX: Afatinib decreases P-glycoprotein expression to promote Adriamycin toxicity of A549T cells. Journal of Cellular Biochemistry 2018;119:414-423.
17 Li D, Zhang XW, Jiang XQ, Yin YJ, Fan Z, Sun CB, Chen XH, Li YH, Liu KX: Protective effects of thalidomide on pulmonary injuries in a rat model of paraquat intoxication. J Inflamm (Lond) 2015;12:46.
18 Sterling T, Irwin JJ: ZINC 15 – Ligand Discovery for Everyone. Journal of Chemical Information and Modeling 2015;55:2324-2337.
19 Joshi SD, More UA, Pansuriya K, Aminabhavi TM, Gadad AK: Synthesis and molecular modeling studies of novel pyrrole analogs as antimycobacterial agents. Journal of Saudi Chemical Society 2017;21:42-57.
20 Xue C, Wang C, Qi L, Qiang M, Sun H, Huo X, Ma X, Liu Z, Ma X, Peng J: Targeting P-glycoprotein expression and cancer cell energy metabolism: combination of metformin and 2-deoxyglucose reverses the multidrug resistance of K562/Dox cells to doxorubicin. Tumour Biology the Journal of the International Society for Oncodevelopmental Biology & Medicine 2016;37:8587-8597.
21 Thomas H, Coley HM: Overcoming multidrug resistance in cancer: an update on the clinical strategy of inhibiting p-glycoprotein. Cancer Control 2003;10:159-165.
22 Kalmanti L, Saussele S, Lauseker M, Müller MC, Dietz CT, Heinrich L, Hanfstein B, Proetel U, Fabarius A, Krause SW: Safety and efficacy of imatinib in cml over a period of 10 years: data from the randomized cml-study iv. Leukemia 2015;29:1123-1132.
23 Hochhaus A, Larson RA, Guilhot F, Radich JP, Branford S, Hughes TP, Baccarani M, Deininger MW, Cervantes F, Fujihara S: Long-Term Outcomes of Imatinib Treatment for Chronic Myeloid Leukemia. N Engl J Med 2017;376:917-927.
24 Agrawal M, Hanfstein B, Erben P, Wolf D, Ernst T, Fabarius A, Saussele S, Purkayastha D, Woodman RC, Hofmann WK: MDR1 expression predicts outcome of Ph+ chronic phase CML patients on second-line nilotinib therapy after imatinib failure. Leukemia 2014;28:1478-1485.
25 Tsuruo T, Iida H, Tsukagoshi S, Sakurai Y: Overcoming of vincristine resistance in P388 leukemia *in vivo* and *in vitro* through enhanced cytotoxicity of vincristine and vinblastine by verapamil. Cancer Research 1981;41:1967-1972.
26 Mickisch GH, Noordzij MA, Vd GA, Gebreamlack P, Köhrmann KU, Mogler-Drautz E, Kupper H, Schröder FH: Dexverapamil to modulate vinblastine resistance in metastatic renal cell carcinoma. Journal of Cancer Research & Clinical Oncology 1995;121:11-16.
27 Dei S, Romanelli MN, Manetti D, Chiaramonte N, Coronnello M, Salerno M, Teodori E: Design and synthesis of aminoester heterodimers containing flavone or chromone moieties as modulators of P-glycoprotein-based multidrug resistance (MDR). Bioorg Med Chem 2017;26:50-64.
28 Martelli C, Coronnello M, Dei S, Manetti D, Orlandi F, Scapecchi S, Novella RM, Salerno M, Mini E, Teodori E: Structure-activity relationships studies in a series of N,N-bis(alkanol)amine aryl esters as P-glycoprotein (Pgp) dependent multidrug resistance (MDR) inhibitors. Journal of Medicinal Chemistry 2011;53:1755-1762.

29 Kaldor SW, Kalish VJ, Davies NJ, Shetty BV, Fritz JE, Appelt K, Burgess JA, Campanale KM, Chirgadze NY, Clawson DK: Viracept (nelfinavir mesylate, AG1343): a potent, orally bioavailable inhibitor of HIV-1 protease. Journal of Medicinal Chemistry 1997;40:3979-3985.
30 Blumenthal GM, Gills JJ, Ballas MS, Bernstein WB, Komiya T, Dechowdhury R, Morrow B, Root H, Chun G, Helsabeck C: A phase I trial of the HIV protease inhibitor nelfinavir in adults with solid tumors. Oncotarget 2014;5:8161-8172.
31 Gottesman MM, Lavi O, Hall MD, Gillet JP: Towards a Better Understanding of the Complexity of Cancer Drug Resistance. Annual Review of Pharmacology & Toxicology 2015;56:85-102.
32 Angelidis C, Kotsialou Z, Kossyvakis C, Vrettou AR, Zacharoulis A, Kolokathis F, Kekeris V, Giannopoulos G: Colchicine Pharmacokinetics and Mechanism of Action. Current Pharmaceutical Design 2018;24:659-663.
33 Li QQ, Cao XX, Xu JD, Chen Q, Wang WJ, Tang F, Chen ZQ, Liu XP, Xu ZD: The role of P-glycoprotein/cellular prion protein interaction in multidrug-resistant breast cancer cells treated with paclitaxel. Cellular & Molecular Life Sciences 2009;66:504-515.
34 Ali MA, Elsalakawy WA: ABCB1 haplotypes but not individual SNPs predict for optimal response/failure in Egyptian patients with chronic-phase chronic myeloid leukemia receiving imatinib mesylate. Medical Oncology 2014;31:279.
35 Fan YF, Zhang W, Zeng L, Lei ZN, Cai CY, Gupta P, Yang DH, Cui Q, Qin ZD, Chen ZS: Dacomitinib antagonizes multidrug resistance (MDR) in cancer cells by inhibiting the efflux activity of ABCB1 and ABCG2 transporters. Cancer Letters 2018;421:186-198.
36 Wang Y, Zong S, Wu L, Zhang Y, Wang Z, Wang Z, Chen B, Cui Y: Evaluation of Multidrug Resistance of Leukemia Using SERS Method for Clinical Application. ACS Appl Mater Interfaces 2018;10:24999-25005.
37 Robey RW, Pluchino KM, Hall MD, Fojo AT, Bates SE, Gottesman MM: Revisiting the role of ABC transporters in multidrug-resistant cancer. Nature Reviews Cancer 2018;18:452-464.
38 Hedley DW, Xie SX, Minden MD, Choi CH, Chen H, Ling V: A novel energy dependent mechanism reducing daunorubicin accumulation in acute myeloid leukemia. Leukemia 1997;11:48-53.
39 Shafiei-Irannejad V, Samadi N, Yousefi B, Salehi R, Velaei K, Zarghami N: Metformin enhances doxorubicin sensitivity via inhibition of doxorubicin efflux in P-gp-overexpressing MCF-7 cells. Chemical Biology & Drug Design 2017;91:269-276.
40 Bonora M, Wieckowski MR, Chinopoulos C, Kepp O, Kroemer G, Galluzzi L, Pinton P: Molecular mechanisms of cell death: central implication of ATP synthase in mitochondrial permeability transition. Oncogene 2015;34:1475-1486.
41 Yang X, Liu K, University DM: Molecular structure and mechanism of P-glycoprotein functions. Drug Evaluation Research 2018;41:1-4
42 Aller SG, Li J, Jaimes K: Refined Structures of Mouse P-Glycoprotein. Protein Science 2013;23:34-46.
43 Kim Y, Chen J: Molecular structure of human P-glycoprotein in the ATP-bound, outward-facing conformation. Science 2018;359:915-919.
44 Martindale JL, Holbrook NJ: Cellular response to oxidative stress: signaling for suicide and survival. J Cell Physiol 2002;192:1-15.
45 Marie Cargnello PPR: Activation and Function of the MAPKs and Their Substrates, the MAPK-Activated Protein Kinases. Microbiology & Molecular Biology Reviews Mmbr 2011;75:50-83.
46 Hers I, Vincent EE, Tavare JM: Akt signalling in health and disease. Cell Signal 2011;23:1515-1527.
47 Liu Z, Zhu G, Getzenberg RH, Veltri RW: The Upregulation of PI3K/Akt and MAP Kinase Pathways is Associated with Resistance of Microtubule Targeting Drugs in Prostate Cancer. Journal of Cellular Biochemistry 2015;116:1341-1349.
48 Wu G, Qin XQ, Guo JJ, Li TY, Chen JH: AKT/ERK activation is associated with gastric cancer cell resistance to paclitaxel. International Journal of Clinical & Experimental Pathology 2014;7:1449-1458.
49 Zhao L, Shan Y, Bing L, Yang L, Li J: Functional screen analysis reveals miR-3142 as central regulator in chemoresistance and proliferation through activation of the PTEN-AKT pathway in CML. Cell Death & Disease DOI:10.1038/cddis.2017.223.